Supporting Information for:

Comparative Atomistic Insights on Apo and ATP-I1171N/S/T in Nonsmall-Cell Lung Cancer

Ambritha Balasundaram and George Priya C Doss *

Laboratory of Integrative Genomics, Department of Integrative Biology, School of BioSciences and Technology, Vellore Institute of Technology, Vellore, Tamil Nadu 632014, India; ambritha.b2020@vitstudent.ac.in (AB); ORCiD iD: https://orcid.org/0000-0003-2856-4687; georgepriyadoss@vit.ac.in (CGPD); ORCiD iD: https://orcid.org/0000-0002-5971-8290

*Correspondence: George Priya C Doss, Laboratory of Integrative Genomics, Department of Integrative Biology, School of Biosciences and Technology, Vellore Institute of Technology, Vellore, India; georgepriyadoss@vit.ac.in

Contents:

Supplementary Table 1. The binding energy and distance between the Mg & ATP of the ATP-bounded ALK WT and I1171N/S/T mutations in all conformations in triplicates. Where T1, T2, and T3 represent triplicate 1, triplicate 2, and triplicate 3. '*' denoted conformation was selected for further process.

ALK-WT-ATP1-T1	**Conformation**	**Distance (Å) Mg - ATP**	**Binding energy (kcal/mol)**
	1*	5.551	-5.9
	2	11.346	-5.9
	3	12.382	-5.9
	4	5.899	-5.9
	5	10.687	-5.9
	6	11.426	-5.8
	7	9.348	-5.8
	8	12.367	-5.8
	9	7.366	-5.8
ALK-WT-ATP1-T2			
	1*	5.536	-6
	2	9.055	-5.8
	3	11.909	-5.8
	4	13.724	-5.8
	5	7.605	-5.8
	6	10.217	-5.7
	7	6.864	-5.6
	8	12.21	-5.6
	9	9.824	-5.6
ALK-WT-ATP1-T3			
	1	11.827	-6.6
	2	11.706	-6.6
	3	11.598	-6.6
	4	12.346	-6.5
	5	9.44	-6.5
	6*	5.881	-6.4
	7	10.689	-6.4
	8	12.42	-6.3
	9	8.887	-6.3
ALK-I1171T-ATP1-T1			
	1	6.861	-6.5
	2*	3.179	-6.5
	3	10.099	-6.5
	4	7.158	-6.3
	5	7.557	-6.3
	6	7.153	-6.3
	7	3.385	-6.2

	8	8.66	-6.1
	9	9.19	-6.1
ALK-I1171T-ATP1-T2			
	1	7.07	-6.6
	2	6.926	-6.6
	3*	2.239	-6.5
	4	9.952	-6.4
	5	3.717	-6.2
	6	3.72	-6.2
	7	7.01	-6.2
	8	7.317	-6.2
	9	7.045	-6.1
ALK-I1171T-ATP1-T3			
	1	13.554	-6.6
	2*	5.065	-6.6
	3	8.234	-6.5
	4	14.275	-6.5
	5	8.339	-6.5
	6	6.15	-6.4
	7	7.823	-6.4
	8	5.101	-6.4
	9	11.269	-6.3
ALK-I1171S-ATP1-T1			
	1*	5.061	-6.1
	2	7.78	-6.1
	3	8.208	-6.1
	4	8.103	-6
	5	8.342	-6
	6	13.632	-6
	7	10.904	-5.9
	8	6.299	-5.9
	9	7.276	-5.8
ALK-I1171S-ATP1-T2			
	1	13.484	-6.3
	2	10.306	-6.3
	3*	5.107	-6.3
	4	8.091	-6.2
	5	12.973	-6.2
	6	6.271	-6.2
	7	13.586	-6.2
	8	13.593	-6.1
	9	8.518	-6.1
ALK-I1171S-ATP1-T3			
	1	13.554	-6.5
	2*	5.065	-6.2
	3	8.234	-6.2

	4	14.275	-6.1
	5	8.339	-6.1
	6	6.15	-6.1
	7	7.823	-6
	8	5.101	-6
	9	11.269	-6
ALK-I1171N-ATP1-T1			
	1	7.743	-6.4
	2	9.348	-6
	3	9.317	-5.9
	4*	6.098	-5.8
	5	5.759	-5.6
	6	9.109	-5.6
	7	5.149	-4.9
	8	9.249	-4.8
	9	8.439	-4.7
ALK-I1171N-ATP1-T2			
	1*	4.821	-6.9
	2	7.747	-6.3
	3	10.616	-6
	4	9.538	-6
	5	5.973	-5.7
	6	9.288	-5.6
	7	8.393	-5.2
	8	10.038	-4.9
	9	10.14	-3.7
ALK-I1171N-ATP1-T3			
	1	9.245	-5.9
	2*	5.013	-5.9
	3	10.512	-5.9
	4	7.309	-5.1
	5	3.413	-5
	6	5.081	-4.3
	7	3.984	-4.2
	8	7.398	-4.1
	9	9.883	-3

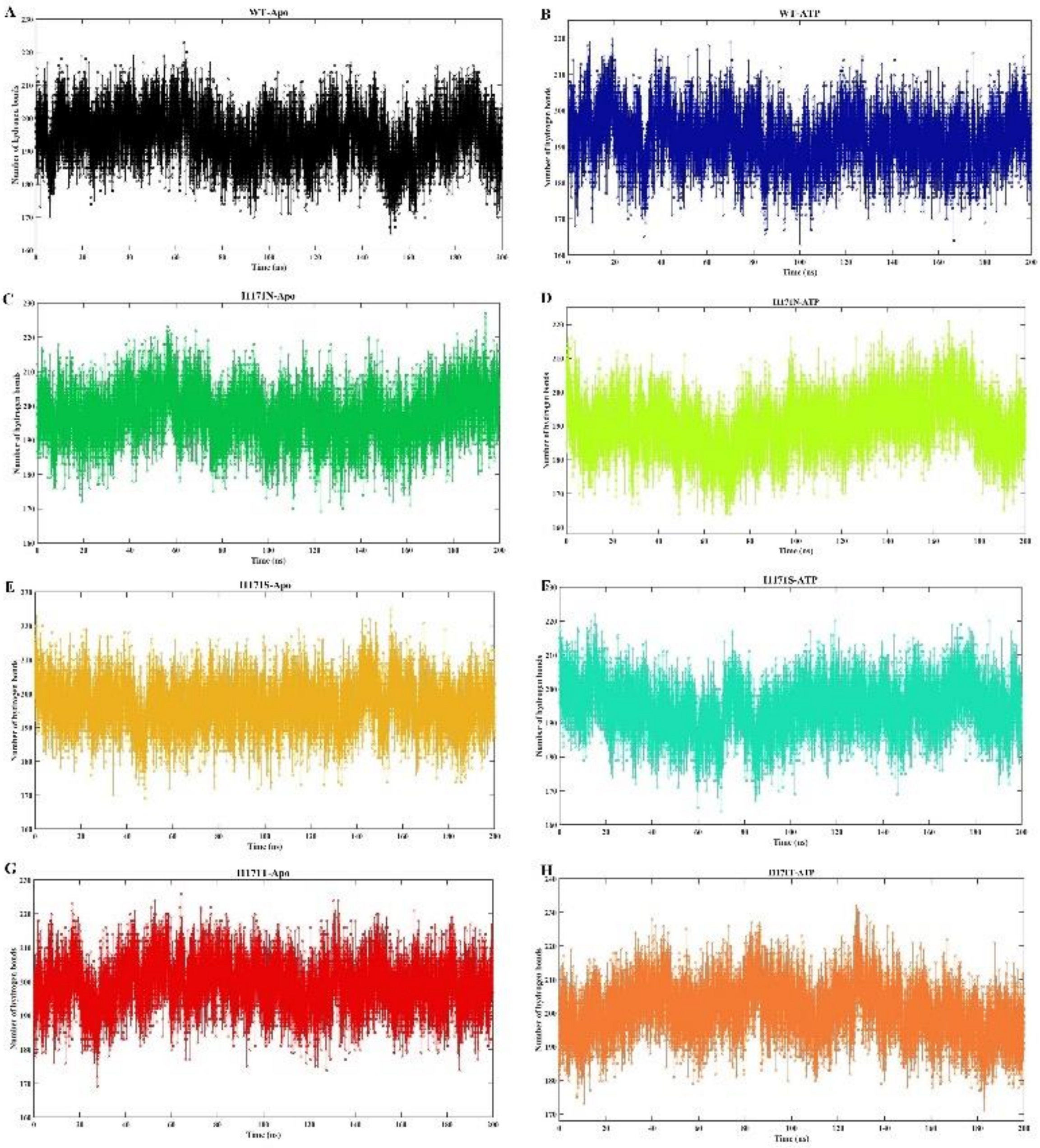

Supplementary Figure 1. The intramolecular hydrogen bond analysis of ALK WT and I1171N/S/T mutations in Apo and ATP bound states. The intramolecular hydrogen bond analysis for (A) WT-Apo showed in black, (B) WT-ATP showed in navy blue, (C) I1171N-Apo showed in green, (D) I1171N-ATP showed in pear, (E) I1171S-Apo showed in mustard, (F) I1171S-ATP showed in cyan, (G) I1171T-Apo showed in red, and (H) I1171T-ATP showed in orange. The X-axis denotes time in ns, and the Y-axis displays H-bonds in number.

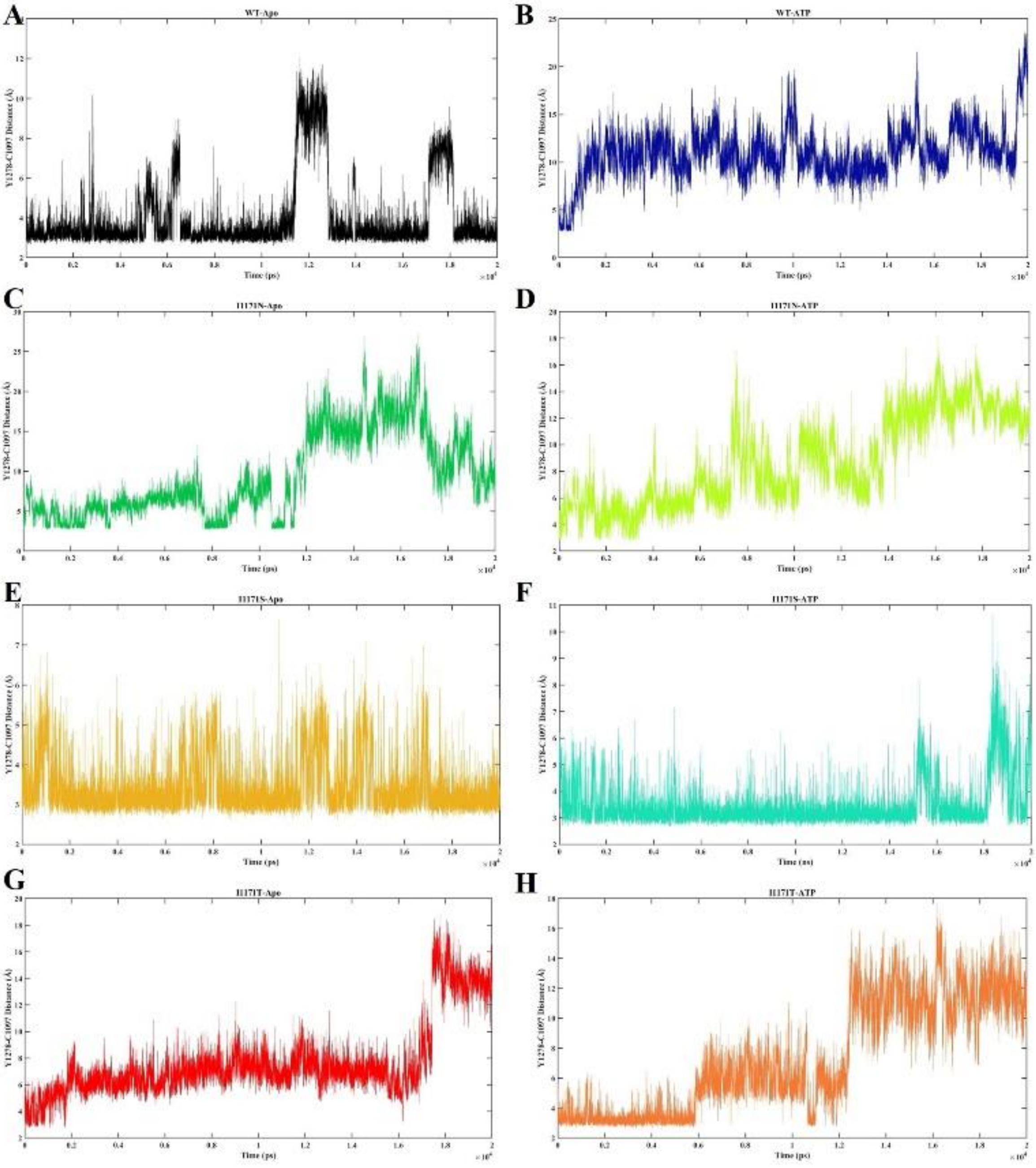

Supplementary Figure 2. The distance between the Y1278 and C1097 of ALK WT and I1171N/S/T mutations in Apo and ATP bound states throughout the MD trajectories. The distance between the Y1278-C1097 for (A) WT-Apo, (B) WT-ATP, (C) I1171N-Apo, (D) I1171N-ATP, (E) I1171S-Apo, (F) I1171S-ATP, (G) I1171T-Apo, and (H) I1171T-ATP. The X-axis denotes time in ps, and the Y-axis displays distance in Å.

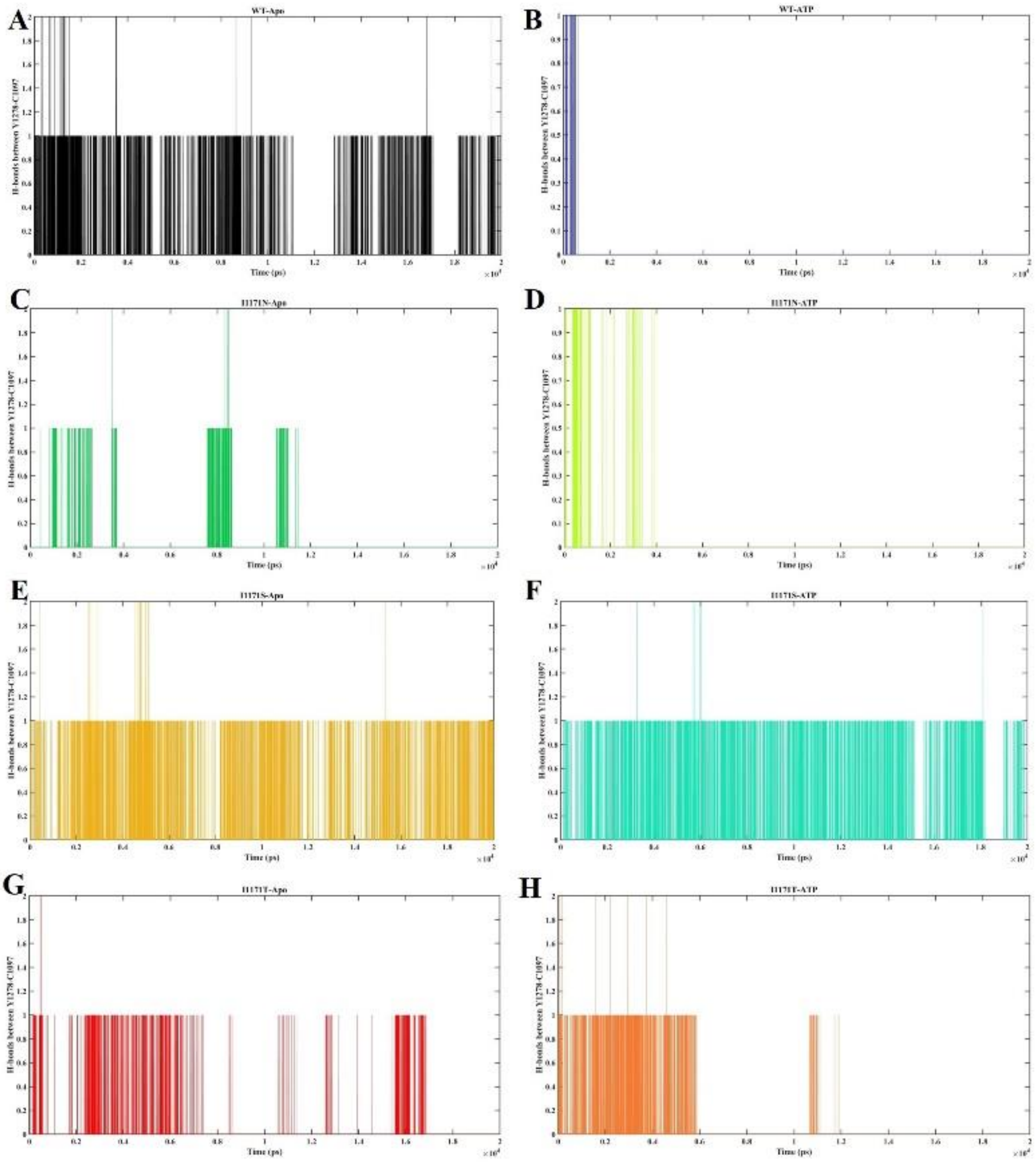

Supplementary Figure 3. The H-bonds formed between the Y1278-C1097 of ALK WT and I1171N/S/T mutations in Apo and ATP bound states. The h-bonds formed between the Y1278-C1097 for (A) WT-Apo, (B) WT-ATP, (C) I1171N-Apo, (D) I1171N-ATP, (E) I1171S-Apo, (F) I1171S-ATP, (G) I1171T-Apo, and (H) I1171T-ATP. The X-axis denotes time in ps, and the Y-axis displays the number of h-bonds formed.

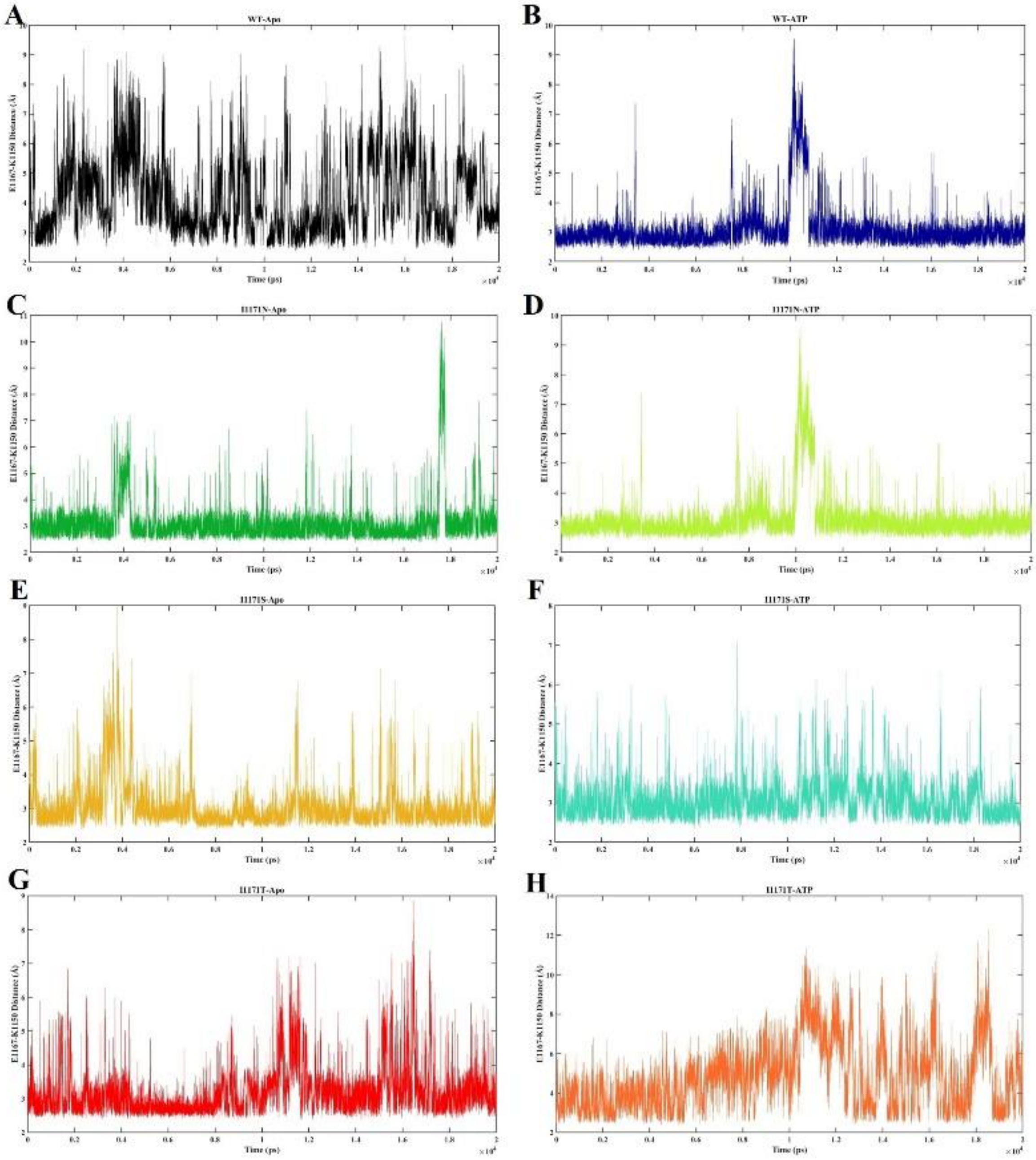

Supplementary Figure 4. The salt bridge distance between E1167-K1150 of ALK WT and I1171N/S/T mutations in Apo and ATP bound states throughout the MD trajectories. The salt-bridge distance between the E1167-K1150 for (A) WT-Apo, (B) WT-ATP, (C) I1171N-Apo, (D) I1171N-ATP, (E) I1171S-Apo, (F) I1171S-ATP, (G) I1171T-Apo, and (H) I1171T-ATP. The X-axis denotes time in ps, and the Y-axis displays distance in Å.

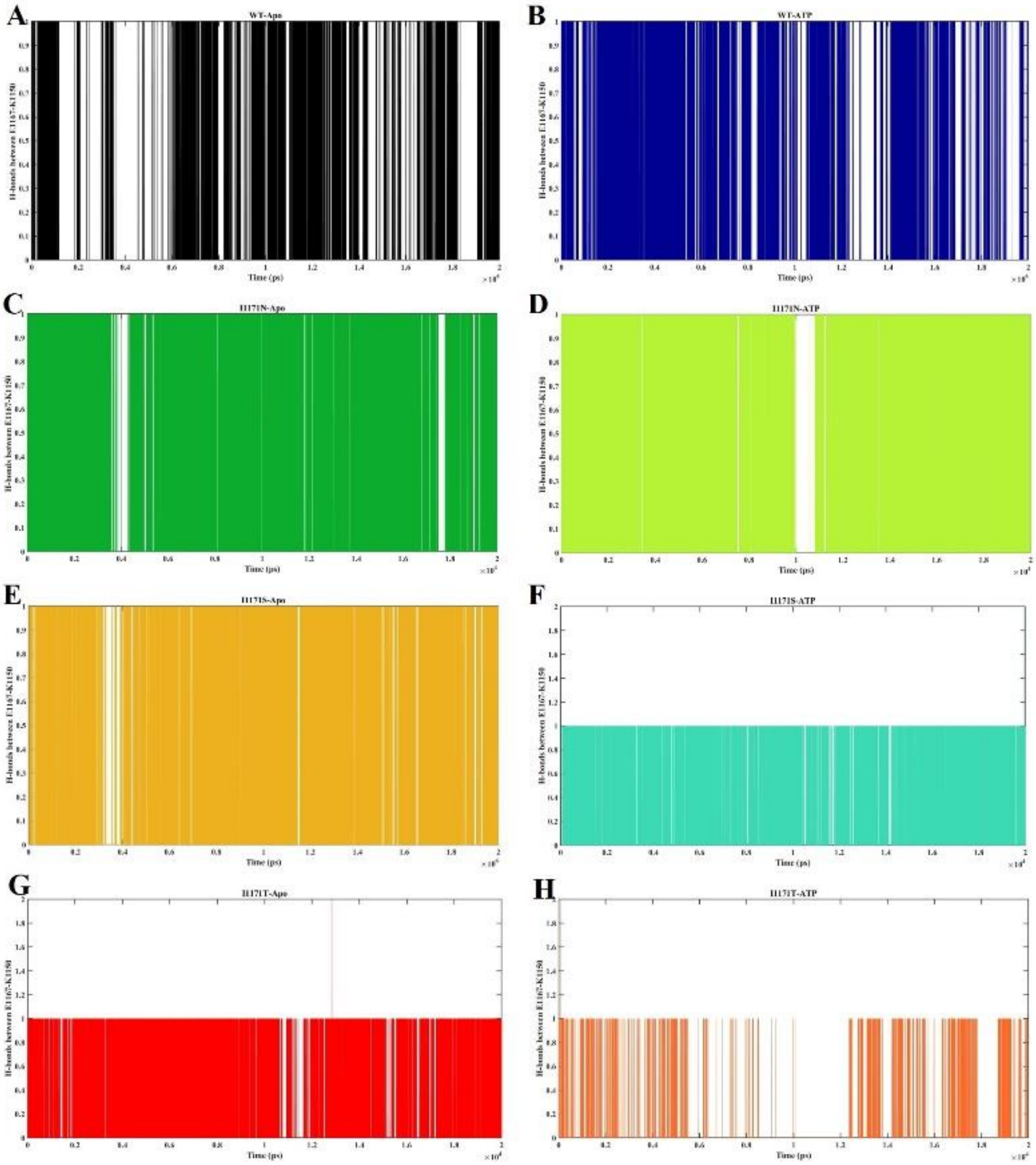

Supplementary Figure 5. The H-bonds formed between the E1167-K1150 of ALK WT and I1171N/S/T mutations in Apo and ATP bound states. The h-bond formed between the E1167-K1150 for (A) WT-Apo, (B) WT-ATP, (C) I1171N-Apo, (D) I1171N-ATP, (E) I1171S-Apo, (F) I1171S-ATP, (G) I1171T-Apo, and (H) I1171T-ATP. The X-axis denotes time in ps, and the Y-axis displays the number of h-bonds formed.

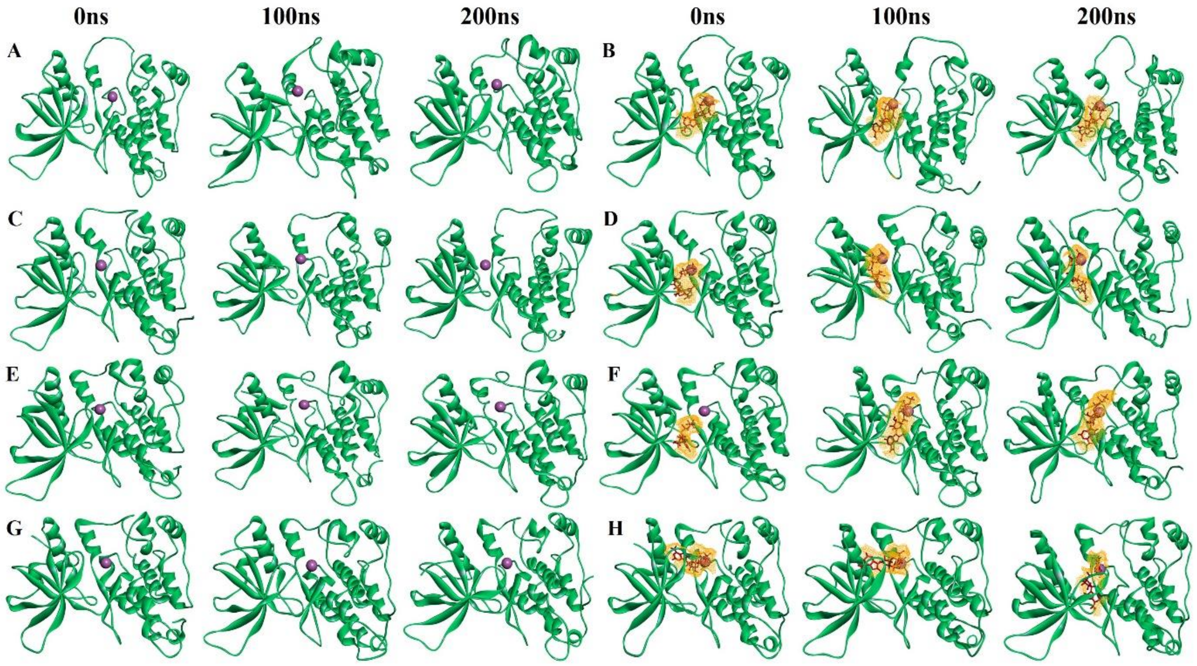

Supplementary Figure 6. The cartoon illustration of snapshots of the structures were extracted from trajectories at 100ns intervals of the ALK WT and I1171N/S/T mutations in Apo and ATP bound states over the entire simulations.

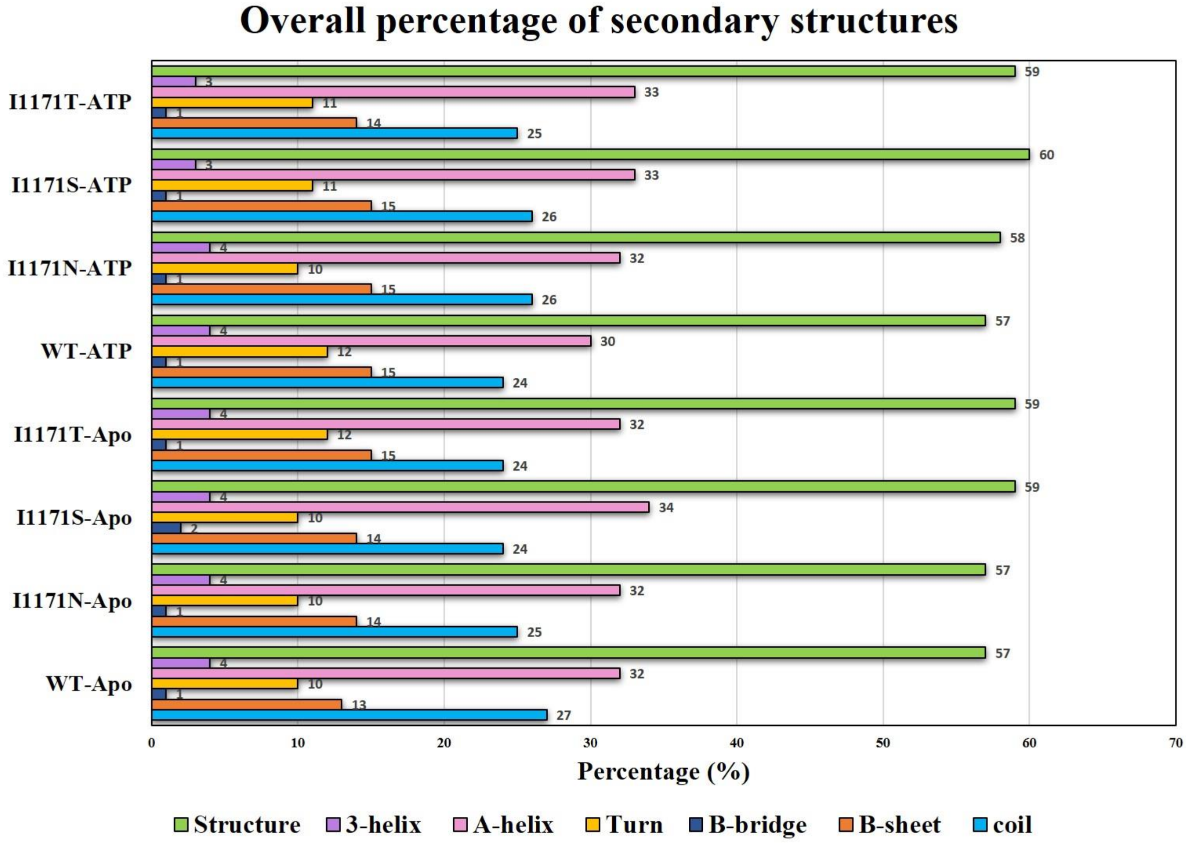

Supplementary Figure 7. The overall percentage of secondary structures for ALK WT and I1171N/S/T mutations in Apo and ATP bound states. The structure includes A-helix, B-sheet, B-bridge, and Turn.